Organic & Biomolecular Chemistry

ROYAL SOCIETY OF CHEMISTRY

PAPER

View Article Online
View Journal | View Issue

Cite this: *Org. Biomol. Chem.*, 2022, **20**, 649

A DFT examination of the role of proximal boron functionalities in the *S*-alkylation of sulfenic acid anions†

Andrew G. Durant, Eric A. Nicol, Brandon M. McInnes and Adrian L. Schwan *

Sulfenic acid anions represent an emerging nucleophile for the preparation of sulfoxides. Their S-functionalization chemistry can often be influenced by a nearby group that interacts with the component atoms of the sulfenate through non-bonding interactions. This study uses DFT methods to assess the importance of proximal boron-containing functional groups to direct *S*-alkylation chemistry of selected sulfenate anions. Several structural variations were modelled at the B3LYP/6-311++G(d,p) level, with the boron species positioned 3 to 5 carbons away from the alkylation site. Transition state free energies of *S*-alkylation transition states were located with and without sulfenate oxygen precomplexing to the nearby boron atom. The outcomes suggest that an *ortho*-substituted boronate ester on benzyl bromide can direct and accelerate an alkylation reaction principally due to a reduction of the entropic barrier. It was also determined that an intermolecular precomplex imparts too much stabilization to the sulfenate, thereby reducing its reactivity. The modelling suggests a possible aryl migration of the boronate/sulfenate complex is not competitive with *S*-alkylation.

Received 24th October 2021,
Accepted 16th December 2021

DOI: 10.1039/d1ob02083h

rsc.li/obc

Introduction

Invention in organic synthesis often requires the recognition and development of new interactions of functional groups and/or reactive intermediates. The ground is often fertile when one brings unexplored functional groups and their associated reactivities together to execute chemistry and such achievements frequently employ combinations of heteroatom containing moieties.[1]

In particular, pairing organosulfur functional groups or reagents with other organoheteroatom containing substrates has unveiled many useful protocols. The combination of sulfur and phosphorus reactivity has produced a version of the valuable Staudinger ligation[2] and is vital to the one-pot synthesis of the theoretically interesting and synthetically useful Sondheimer–Wong cyclic diynes.[3] In the realm of sulfur and silicon reactivity, the use of a strategically silyl- and sulfonyl-substituted carbon atom facilitates selective C–C bond formation through an anion relay process to grant access to the 5-membered ring of prostaglandin E2.[4]

The application of sulfur chemistry to the rapidly expanding field of organoboron chemistry has proved fruitful, with a number of valuable applications disseminated. For instance, the sulfinyl group can direct the borane based reduction of alkenes.[5] The sulfinyl group of a sulfinylimine also directs stereoselective borylation reactions eventually leading to α-amino[6] and β-amino[7] boronic acid derivatives. The Aggarwal group has employed sulfoxides as a clean source of organometallic reagents, which in turn were reacted with boronic esters for the eventual formation of substituted cyclobutyl[8] and azetidinyl[9] boronates. This strategy was also adopted for the stereoselective iterative construction of boronic esters.[10] Lo and Willis demonstrated the Ni-catalyzed reaction of (het)aryl boroxines and trityl sulfinylamine to create metalated sulfinamides, which in turn can be treated further to produce sulfinamides, sulfonamides, sulfonimidamides, and sulfonimidoyl halides.[11]

There are several reports of combining the Lewis acidity of the trivalent boron and Lewis basicity of sulfinyl groups. Tobrman explored the use of complexes possessing internal sulfinyl oxygen-to-boron coordination as bench stable derivatives of the MIDA group.[12] Hattori and coworkers found that Et_3B can assist in controlling the isomeric outcome during the preparation of sulfinylcalix[4]arenes through an O → B interaction.[13]

Also founded on the Lewis acid/base interaction of a sulfinyl oxygen and a boron, the borane-based deoxygenation of

Department of Chemistry, University of Guelph, Guelph, Ontario, Canada N1G 2 W1. E-mail: schwan@uoguelph.ca

†Electronic supplementary information (ESI) available: Optimized structure images, NBO orbital images, table of optimized structural parameters, xyz coordinates and energies of optimized structure. See DOI: 10.1039/d1ob02083h

sulfoxides has been known for some time,[5,14] and in 2020, a new version was introduced by the Yorimitsu group.[15] In that work, an initial sulfinyl oxygen/boron coordination between sulfoxide and one boron of B_2cat_2 is followed by thermally induced migration of the other Bcat to oxygen with concomitant cleavage of the S–O bond. This method represents a non-halo, non-metal protocol for sulfoxide deoxygenation (Scheme 1a).

A related example from Liu and Benkovic[16] invokes the interaction of a different oxygenated sulfur species and a boron. They investigated the reversible complexation of the oxygen of a sulfenate anion with the boron atom of boronic acids and a benzoxaborole (Scheme 1b). That a sulfenate oxygen adds to boronic acid derivatives to make a tetrahedral boron was confirmed by ^{11}B NMR. The work also demonstrated a model reaction to capture biological sulfenate and inhibit the bioactivity of oxidized cysteine residues. The study represents the first report of an R–S–O–B connection.[16]

As researchers who explore the alkylation chemistry of sulfenate anions,[17] the chemistry unveiled by the Benkovic group suggested to us that a proximal boron group may have an influence on the *S*-alkylation chemistry of selected halide electrophiles. Specifically, it was hoped an initial complexation of the sulfenate oxygen to the boron would direct and hopefully accelerate the *S*-alkylation chemistry (Scheme 1c). In this work we explore such interactions on a variety of substrates using DFT-based computational methods. From this study, we predict that selected borylated alkyl and benzyl bromides will undergo more rapid S-functionalization when ring size considerations are met, and boron substituents are amenable. The outcomes grow our understanding of the role of proximal functionalities in guiding sulfenate reactivity and will also direct synthetic chemists toward viable, selective sulfoxide syntheses.

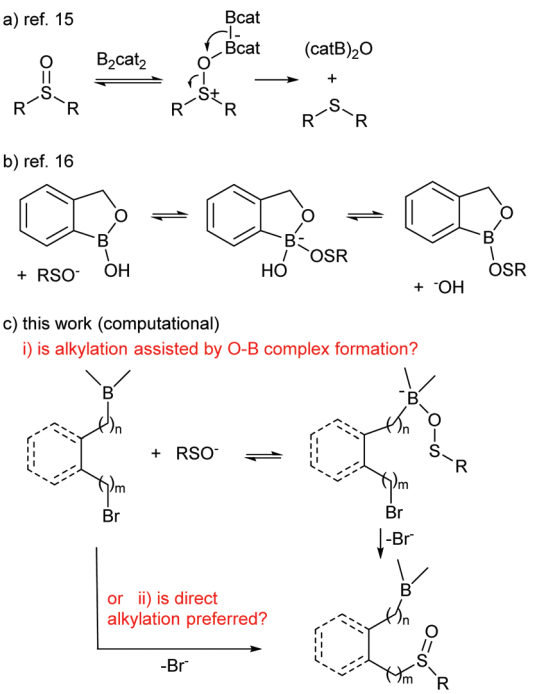

Scheme 1 Sulfur oxygen interactions with boron compounds (n = 0–2; m = 1–3).

Computational details

Optimization and frequency calculations were performed using the Gaussian 16 software package[31] using the B3LYP DFT functional[18] with a 6-311++G(d,p) basis set for all atoms, employing an ultrafine grid. The inclusion of polarization and diffuse functions was chosen to ensure accurate representation of the energy of the sulfoxide relative to the sulfenate, as shown by Turecek[19] and Cubbage,[20] and for accurate modelling of the anionic sulfenate. Implicit solvation with THF was performed through application of the CPCM model.[21] Transition states were identified through the presence of a single negative frequency and confirmed through intrinsic reaction coordinate (IRC) calculations. Minima were confirmed through the absence of a negative frequency. Natural bond orbital (NBO)[22] analysis second-order perturbation was performed using the NBO6[32] program on select transition states for quantification of hyperconjugative effects. QTAIM analyses were performed using AIM2000 version 1.0.[23]

Results and discussion

Studies were undertaken employing either methanesulfenate anion ($MeSO^-$) or benzenesulfenate (phenyl sulfenate, $PhSO^-$, **1**) as the standard sulfenate species. A proximal metal counterion was not included for simplicity reasons; such conditions represent a model for the use of tetraalkylammonium counterions[24] or conditions when a metal counterion has been sequestered.[17a]

Recognizing the ambiphilic nature of the sulfenate functional group, the chosen starting point was to confirm that sulfenate O → B coordination was preferred over S → B. Using methanesulfenate the complexation energies were found for optimized structures possessing both modes of complexation to four representative boron derivatives, $PhB(OH)_2$, BMe_3, BF_3, and the ethylene glycol ester of methylboronic acid, MeB(EG). As shown in Table 1 (entries 1–4), coordination of oxygen to boron demonstrates a clear preference over sulfur, with energy differences of at least 9.6 kcal mol^{-1} in all cases. Trends based on variation of the boron substrate are generally consistent with the known Lewis acidity trends of these and related compounds.[25]

Additionally, the coordination chemistry of MeB(EG) and Me_3B was explored employing lithiated and potassiated versions of methanesulfenate. Optimized complexes (Table 1, entries 5–8) still exhibited a clear but slightly attenuated preference for oxygen coordination over sulfur; however, the overall energetic benefits of complexation were either weaker (entry 8) or lost (entries 5–7). These data emphasize the impor-

Table 1 Coordination energy preferences of methanesulfenate with selected boron compounds

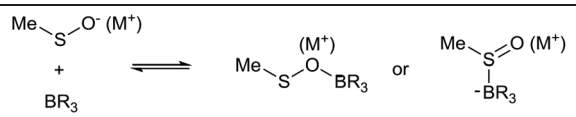

Entry	B species	M^+	ΔG(O–B)[a]	ΔG(S–B)[a]	$\Delta\Delta G$
1	MeB(EG)	—	−0.5	13.8	−14.3
2	$PhB(OH)_2$	—	−4.5	11.8	−16.3
3	BMe_3	—	−7.3	2.3	−9.6
4	BF_3	—	−42.2	−17.0	−25.2
5	MeB(EG)	Li^+	3.2	(14.6)[b]	(−11.4)[b]
6	MeB(EG)	K^+	2.1	15.3	−13.1
7	BMe_3	Li^+	1.6	7.4	−5.8
8	BMe_3	K^+	−2.1	4.9	−7.1

[a] Values represent free energies (kcal mol^{-1}) of optimized structures relative to the separated reactants, optimized with B3LYP/6-311++G(d, p); implicit solvation *via* CPCM(THF). [b] A local minimum for sulfur coordination of lithium methanesulfenate to MeB(EG) could not be located; optimization rendered a species with Li bridging between the sulfenate oxygen and an oxygen of the boronate ester (ΔG = + 5.3 kcal mol^{-1} *vs.* starting materials). The entry of 14.6 kcal mol^{-1} on entry 5 of Table 1 represents an optimized S → B complex with the r(S–B) interatomic distance frozen at 2.183 Å.

tance of utilizing the metal ion free sulfenates to ensure the most powerful O → B interactions and directing effects.

In the metal free conditions, these findings confirm the noteworthy preference for oxygen complexation over sulfur and are consistent with the mode of complexation proposed by Benkovic.[16] For our purposes, this preferential complexation of boron with the sulfinyl oxygen leaves the lone pairs of electrons on sulfur available for nucleophilic chemistry, as per Scheme 1. Moving forward, the reaction of phenyl sulfenate ($PhSO^-$, **1**) with 2-[2-(bromomethyl)phenyl]-1,3,2-dioxaborolane (**2a**, Fig. 1) forms the basis of several comparative investigations. Boronic ester **2a** presents an opportunity for sulfenate O → B coordination and positions a reactive benzyl bromide nearby for sulfoxide formation by *S*-alkylation.

To understand the role of the *ortho* substituted boronate, the initial study incorporated two comparative benzylating agents: benzyl bromide (**2**) representing the parent electrophile and 2-isopropyl benzyl bromide (**2iP**), a presumed steric equivalent of **2a**. Transition states for sulfenate sulfur substitution on the bromides were found, including two of similar energy for **2iP** (**1·2iP·TSa** and **1·2iP·TSb**). Two suitable transition states for **2a** were also found (**1·2a·C·TS** and **1·2a·TS**), one occurring from a sulfenate O → B precomplex (**1·2a·C**) and another with the sulfenate oxygen intentionally directed away from engagement with the boron of **2a**. Relative free energies of the reactions are assembled in Fig. 2. All boron complexed *S*-alkylation transition states are shown in Fig. 3. All *S*-alkylation transition states are shown in Table S1 (ESI).† Thermodynamic parameters and coordinates for all optimized structures are also found in the ESI.† (Key to molecule numbering: first two entries are interacting entities; '**C**' designates O → B coordination; '**TS**' designates transition state.)

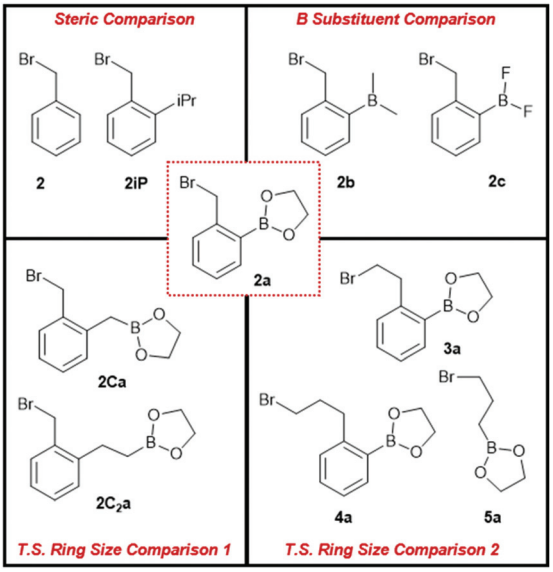

Fig. 1 Electrophiles evaluated for reaction with phenyl sulfenate ($PhSO^-$, **1**).

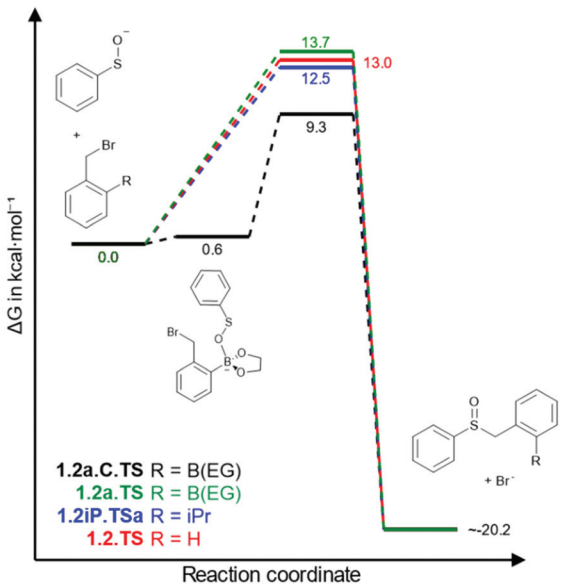

Fig. 2 Comparative free energies of sulfenate reactions with *o*-substituted benzyl bromides calculated at B3LYP/6-311++G(d,p), implicit solvation *via* CPCM(THF). (**1·2iP·TSb** has been excluded. It was 12.7 kcal mol^{-1} above starting materials).

Several items are noted from the comparative data. The transition state free energies are comparable near 13 kcal mol^{-1} for the substitution of **1** on **2** (**1·2·TS**), **2iP** (**1·2iP·TSa**) and also on **2a** when no O → B precomplexation is in place (**1·2a·TS**). In contrast, O → B complex **1·2a·C** only requires a small free energy increase for formation, and the internal sulfenate substitution pathway is lower by 3.2–4.4 kcal mol^{-1}; after complexing to the B, the barrier for sulfoxide formation is 8.7 kcal mol^{-1}. At this point the incorporation of one explicit

THF molecule was evaluated for its role in influencing the sulfenate oxygen coordination. It was quickly learned that the THF did not display any affinity for the B atom in either the boronate ester **2a** or the ethylene glycol ester of phenylboronic acid under the model chemistry employed; this was not pursued further.‡

Changing boron substituents to Me and F lowers the barrier for uncomplexed sulfenate substitution slightly. More importantly, the O → B precomplexation imparts sulfenate stabilization when Me and F represent the groups on boron. Fig. 4 demonstrates **1** has a lower energy interaction with **2b** and **2c**, as predicted from the preliminary work (Table 1), and accordingly, the transition state free energy barriers of **1·2b·C·TS** and **1·2c·C·TS** are also lowered (Fig. 4). Of particular note is the potential energy surface (PES) of **1** reacting with **2b** which requires a comparatively small free energy barrier of ~6 kcal mol^{-1} to complete the substitution from its precomplex (**1·2b·C**). O → B formation of difluorinated **2c** is highly stabilizing, and sulfoxide formation requires 10.8 kcal mol^{-1}. In all cases the precomplexed sulfenate has a lower free energy barrier than the respective uncomplexed analog.

Further adaptions to the molecules under study were centered around the use of the ethylene glycol derived boronic ester **2a**. The boronic ester of **2a** serves as a model for the popular and stable Bpin functional group. Boronic esters also demonstrate vast synthetic value in organic chemistry.[26]

The importance of the proximity of the boronic ester was examined by placing intervening methylene groups between the aryl ring and the boronic ester. Accordingly, boronates **2Ca** and **2C$_2$a** (Fig. 1) were subjected to sulfenate substitution with and without prior O → B coordination. Fig. 5 shows the PES's of the possible sulfenate substitution pathways for these compounds alongside those of **1·2a·C·TS** and **1·2a·TS**. Consistent with earlier work, the substitutions that occur without precoordination proceed with a free energy barrier near 12–13 kcal mol^{-1}. However, extending the carbon chain and invoking O → B complex formation prior to sulfenate substitution does not always provide an energetic benefit. As already shown above, formation of complex **1·2a·C** leads to an energetically more favourable transition state. The free energy barrier for the reaction of **1** with **2Ca** is about 13 kcal mol^{-1} whether there is a precomplex or not. Precomplexation of **1** with **2C$_2$a** is actually deleterious for sulfenate substitution, requiring an additional free energy barrier of 16.2 kcal mol^{-1} (17.4 kcal mol^{-1} overall from separated reactants).§

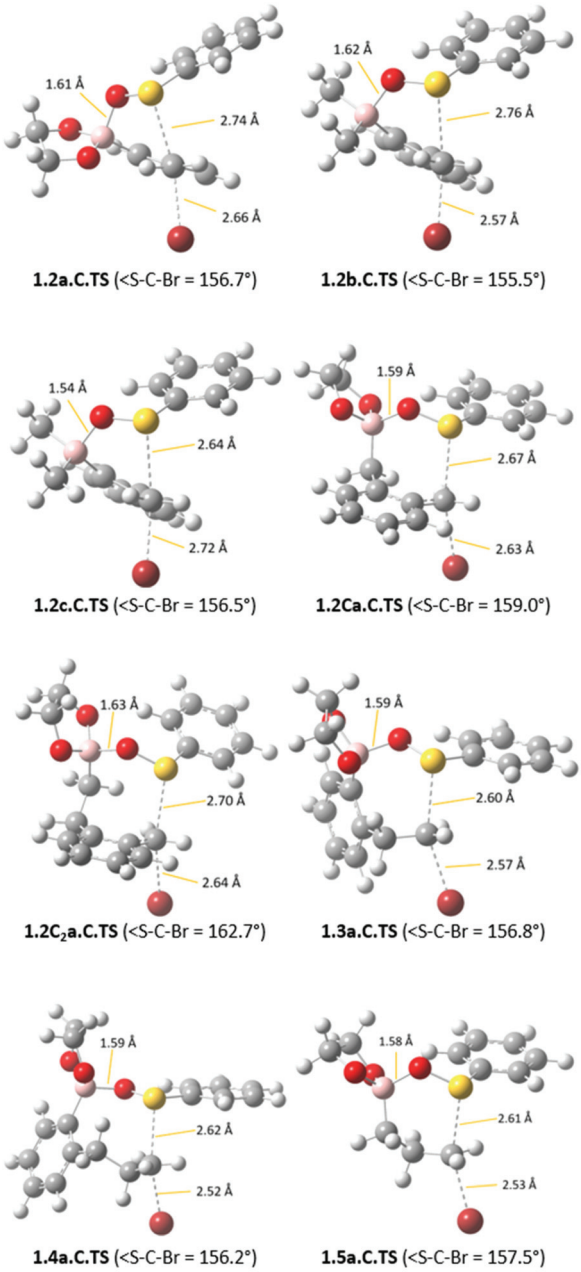

Fig. 3 Transition states of boron precomplexed *S*-alkylations optimized with B3LYP/6-311++G(d,p); implicit solvation *via* CPCM(THF).

Entries 1–6 in Table 2 break down the energetics for these three systems. In the instances where no precomplexation is modelled, the enthalpy of activation is +2–3 kcal mol^{-1} and the entropy of activation ranges between −34 to −36 e.u. On the other hand, the complexation enthalpy is consistently beneficial by −11.6 kcal mol^{-1}, whereas the entropy changes range from −41 to −45 e.u. From the complex to alkylation transition state, the enthalpy of activation increases from +7.3 to +13.9 kcal mol^{-1} as the ring size increases and is responsible for most of the free energy barriers; the entropy of activation change trend is not linear but culminates with a high of

‡ Prompted by a referee, we explored representative systems employing Grimme's D3 dispersion correction.[33] The overall energies were lowered for sulfenate coordination to boron, but the relative S *vs.* O preferences exhibited minimal change. The energies relating to selected potential energy surfaces of Fig. 2 were similarly lowered relative to starting materials but the relative transition state energies for coordinated (**1·2a·C·TS**) *vs.* non-coordinated (**1·2a·TS**) benzylations varied only slightly (4.4 (Fig. 2) *vs.* 4.9 kcal mol^{-1} with D3). The lower overall energies with D3 may be an overstabilization. See ref. 34.

§ Computational control studies of **2a**, **2C$_2$a** and **4a** revealed that internal Br → B interaction was not an important consideration.

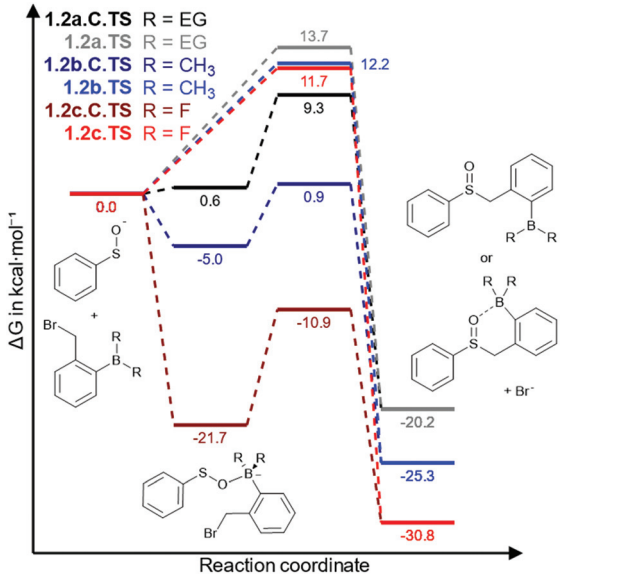

Fig. 4 Comparative free energies of sulfenate reactions with *o*-borylated benzyl bromides calculated at B3LYP/6-311++G(d,p); implicit solvation *via* CPCM(THF).

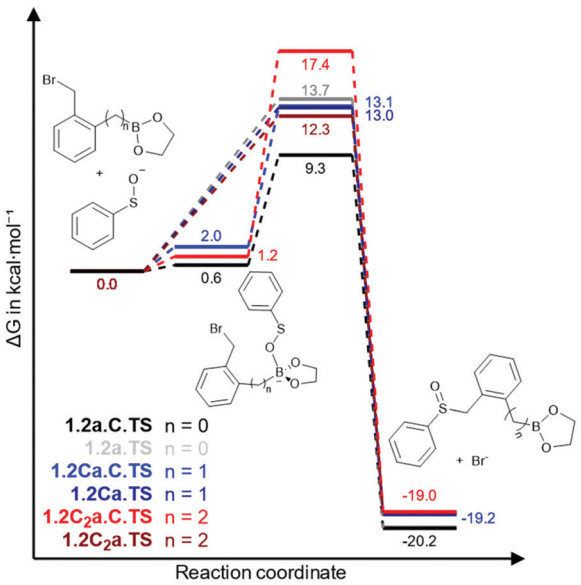

Fig. 5 Comparative free energies of sulfenate reactions with proximally borylated benzyl bromides calculated at B3LYP/6-311++G(d,p); implicit solvation *via* CPCM(THF).

−7.8 e.u. for the 8-membered transition state of **1·2C$_2$a·C·TS.** Overall, these data suggest formation of an enthalpically advantageous precomplex helps to overcome a substantial component of the entropic barrier for the overall substitution reaction. The alkylation rate thereafter is governed mostly by an enthalpic barrier that becomes of greater importance with increasing transition state ring size.

Employing the reaction of **1** and **2a** once again as the comparative standard, precomplexes and sulfenate displacement transition states were sought for bromides **2a**, **3a** and **4a.** Energy levels for this series of sulfenate benzylations are shown in Fig. 6. In the instances of sulfenate substitution with deliberate absence of coordination, reactions have a higher barrier when the Br atom is not at the benzyl position, consistent with recognized substitution reactivity.[27] The O → B coordination complexes all possess higher free energy positions when the Br is moved away from the benzyl position (Table 2, entries 7, 9 and 11; Fig. 6) and the enthalpic benefit is not as significant. It is also noted that the $\Delta H^{\ddagger}$ and $\Delta G^{\ddagger}$ values for cyclization of the complexes are greater compared to the other ring-size variation models addressed above (Table 2, entries 3 and 5; Fig. 6) The 2-step complexation/substitution

Table 2 Activation parameters for precomplexed and uncomplexed sulfenate substitutions

Entry	System	$\Delta G^{\ddagger a}$	$\Delta H_c{}^{a,c}$	$\Delta H_r{}^{\ddagger a,c}$	$\Delta S_c{}^{b,c}$	$\Delta S_r{}^{\ddagger b,c}$
1	**1·2a·C**	8.7	−11.6	−4.4(7.3)[d]	−40.9	−45.7 (−4.8)[e]
2	**1·2a**	13.7	—	2.9	—	−36.0
3	**1·2Ca·C**	11.1	-11.5	−1.4(10.1)[d]	−45.2	−48.2(−3.0)[e]
4	**1·2Ca**	13.0	—	2.2	—	−36.2
5	**1·2C$_2$a·C**	16.2	−11.6	2.3(13.9)[d]	−42.9	−50.7(−7.8)[e]
6	**1·2C$_2$a**	12.3	—	2.2	—	−33.9
7	**1·3a·C**	14.5	−8.4	4.9(13.3)[d]	−42.9	−46.9(−4.1)[e]
8	**1·3a**	16.8	—	6.2	—	−35.5
9	**1·4a·C**	19.6	−9.6	8.3(17.8)[d]	−42.9	−48.9(−6.0)[e]
10	**1·4a**	19.9	—	8.6	—	−37.7
11	**1·5a·C**	15.5	−10.2	4.5(14.7)[d]	−44.3	−46.8(−2.5)[e]
12	**1·5a**	15.2	—	4.5	—	−35.9

[a] Units: kcal mol^{-1}. $\Delta G^{\ddagger}$ is for the alkylation chemistry regardless of the immediate precursor. [b] Units: cal (mol K)$^{-1}$. [c] Subscripted 'r' is for the alkylation reaction. Subscripted 'c' is for the complex formation. [d] Parenthesized value represents the enthalpy difference going from complex to alkylation transition state. [e] Parenthesized value represents the entropy difference going from complex to alkylation transition state.

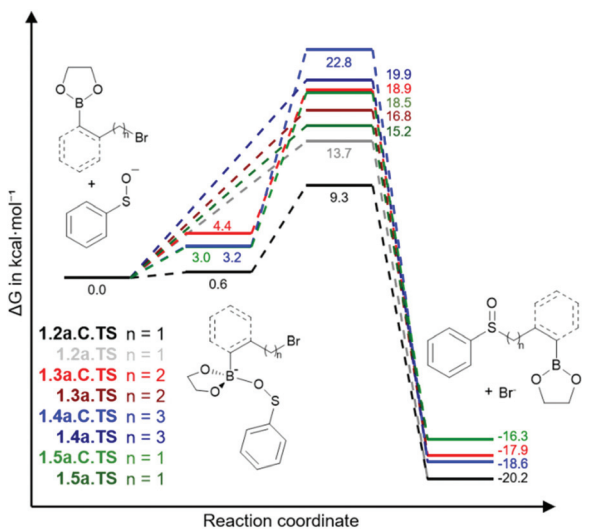

Fig. 6 Comparative free energies of sulfenate reactions with alkyl bromides bearing pendant *o*-borylated phenyl groups calculated at B3LYP/6-311++G(d,p); implicit solvation *via* CPCM(THF).

sequence does not seem to provide an energetic benefit over the direct substitution pathway.

Table S1 (ESI)† portrays a collection of key geometric parameters for the sulfenate substitutions. The key elements of change during the substitution reaction are addressed here. The *r*(S–O) bond length is 1.608 Å in the free benzenesulfenate (**1**). This parameter shortens by 0.024–0.031 Å in the transition state for direct sulfoxide formation, an observation that has been noted in the past.[28] If the sulfenate oxygen first interacts with the boron, the *r*(S–O) of the adducts lengthens to 1.652–1.661 Å. In the *S*-alkylation transition states for the complexed sulfenates, the *r*(S–O) reduces by a comparable 0.024–0.030 Å. There is a corresponding change in the *r*(O–B) interatomic distance also. Initially, the complexes possess *r*(O–B) ranging from 1.505–1.585 Å, with the ethylene glycol based boronate complexes consistently in a tighter range, 1.550–1.569 Å. As the complex goes through the alkylation transition state, the *r*(O–B) interaction is maintained but the interatomic distance lengthens by as much as 0.060 Å (**1·2C$_2$a·C·TS**) or by as little as 0.014 Å (**1·5a·C·TS**).¶

The complexed and uncomplexed transition states display contrasting *r*(S–C) and *r*(C–Br) interatomic distances. Generally, the direct uncomplexed transition states exhibit *r*(S–C) interatomic distances of 2.805–2.974 Å for the bromide displacement reaction and 2.351–2.495 Å for *r*(C–Br) interatomic distances of the same transition states. The *r*(S–C) and *r*(C–Br) distances in the precomplexed transition states are 2.601–2.761 Å and 2.516–2.721 Å, respectively. The transition states of the uncomplexed sulfenate alkylations display longer *r*(S–C) values and shorter *r*(C–Br) distances suggesting they proceed through a less-advanced and earlier transition state, which was corroborated through inspection of the intrinsic reaction coordinates of the computed transition states. However, examining the two **1·2a** pathways, where the complex (**1·2a·C**) is slightly higher in energy, but has a lower transition state for benzylation, the differences suggest a beneficial O → B complexation is accelerating the substitution, but with a later, more advanced transition state.

The geometries of the uncomplexed transition states for Br substitution at the non-benzylic position (**1·3a·TS**, **1·4a·TS**, **1·5a·TS**) all exhibited an unexpected feature. There appeared to be hydrogen bonding of the sulfenate oxygen with the H β to the bromide. This was confirmed by QTAIM calculations wherein applicable bond critical points were identified,[23] and by NBO calculations (Table 3). To learn more about the significance of the H-bonding effect, we successfully found transition states for substitution on **4**/**5**/**6a** wherein the sulfenate oxygen was directed away from the β-H (and from the B), and these transition states are labelled as **1·3a·TS2**, **1·4a·TS2**, **1·5a·TS2**. Transition state images for **1·3a·TS** and **1·3a·TS2** are shown in Fig. 7, while all examples and applicable NBO images are found in the ESI.†

Table 3 Selected structural parameters of optimized *S*-alkylation transition states

	$\Delta G^{\ddagger a}$	r(O···H)^b	r(S–C)^b	r(C–Br)^b	ρ^c	E [$\sigma_{C-H} \rightarrow \sigma^*_{C-Br}$]^a
1·3a·TS	16.8	1.948	2.805	2.495	0.031	14.8^d
1·3a·TS2	19.6		2.714	2.471		9.6^e
1·4a·TS	19.9	2.076	2.805	2.477	0.024	12.1^d
1·4a·TS2	21.7		2.722	2.438		7.0^e
1·5a·TS	15.2	2.020	2.815	2.477	0.026	13.7^d
1·5a·TS2	17.5		2.712	2.436		8.6^e

[a] Units: kcal mol^{-1}. [b] Units: Å. [c] The electron density at the bond critical point. See ref. 23. [d] Energy of primary hyperconjugation at alkylation transition state in the presence of O···H interaction. [e] Stabilization energy of hyperconjugation in the absence of sulfenate oxygen engagement.

From a free energy perspective, the apparent H-bond stabilization is worth 1.8–2.8 kcal mol^{-1}. NBO assessments indicate the H-bonding is actually integrated with [$\sigma_{C-H} \rightarrow \sigma^*_{C-Br}$] hyperconjugation, which lengthens the C–Br bond and in turn, accelerates the alkyl transfer to the sulfenate. The H-bond/hyperconjugative combination of **1·3a·TS** is preferred by 2.7 kcal mol^{-1} over that of **1·4a·TS**, thus identifying the principal origin of the transition state energy difference (*cf.*, 2.8 kcal mol^{-1}). A visualization of the orbitals involved in these transition states is shown in the ESI.†

This computational discovery is important in light of the reduced reactivity of alkyl halides compared to benzyl halides during sulfenate displacements.[17b] The absence of a metal counterion in this study presumably maximizes the H-bonding interaction, since the metal ion would normally accompany the sulfenate oxygen in ethereal solvents and reduce the strength of the H-bond. A measure support for this premise was obtained from the optimized transition state of **1·4a·TS** holding a single Li^+ counterion on the oxygen (ESI†). That structure demonstrated a *r*(O···H) of 2.210 Å, longer than the 2.076 Å of the non-lithiated version. From a practical point of view, this work suggests that sulfenate alkylation chemistry may be enhanced when the metallic counterion is not proximal, possibly through metal anion sequestration or use of a tetraalkylammonium counterion, thereby freeing the oxygen to participate in H-bonding-based acceleration of the *S*-alkylation.

As a final assessment of the role of boron species possibly facilitating sulfenate *S*-alkylation, we explored the importance of several boron species not tethered to the alkylating agent. In this role, the possibility of complexation of sulfenate oxygen to boron could play a catalytic role in accelerating (or hindering) sulfenate substitution. In this study, benzenesulfenate (**1**) was *S*-alkylated with methyl bromide (**8**) in the absence of a boron species, as the standard. Then we introduced boron entities

¶With a few exceptions, sulfoxides do not stay complexed in the overall product. The exceptions: the diflouro system based on **1·2c** displayed a tetrahedral boron with an O–B distance of 1.593 Å and the dimethyl system (**1·2b**) exhibited a boron between tetrahedral and trigonal planar geometries with an O–B distance of 1.702 Å. The other sulfoxides had a trigonal planar boron. Some intrinsic reaction coordinate plots (to sulfoxide product) demonstrated a small shoulder *after* S–C bond formation caused by the sulfoxide oxygen separating from the boron, see ESI† for IRC of **1·2Ca·C·TS**.

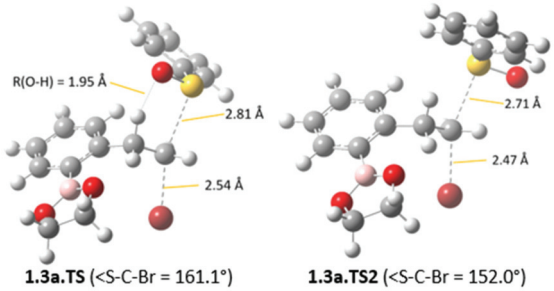

Fig. 7 *S*-Alkylation transition state structures with contrasting H-bonding arrangements optimized with B3LYP/6-311++G(d,p); implicit solvation *via* CPCM(THF).

$PhB(OCH_2)_2$ (**6a**), $PhBMe_2$ (**6b**) $PhBF_2$ (**6c**), and BMe_3 (**7**), and investigated the bimolecular alkylation chemistry of the O → B complexes. The relative free energies of these complexes and associated methylation transition states are presented in Fig. 8.

Apart from **1·6a·C**, each complex lowered the overall free energy of the sulfenate entity, and which was followed by a free energy methylation barrier of 20–22 kcal mol^{-1} which is notably higher than the direct sulfenate methylation transition state barrier of 14.2 kcal mol^{-1}. The lowest barrier for alkylation among the boron associated sulfenates arises from trimethyl borane. Given the boron substituents and model chemistry chosen for the computations, these intermolecular systems indicate that coordination to an intervening boron species retards the rate of *S*-alkylation. It is also important to note these relative free energy values (Fig. 8) underscore the significance of the entropy benefit of O → B precoordination for the systems studied earlier.

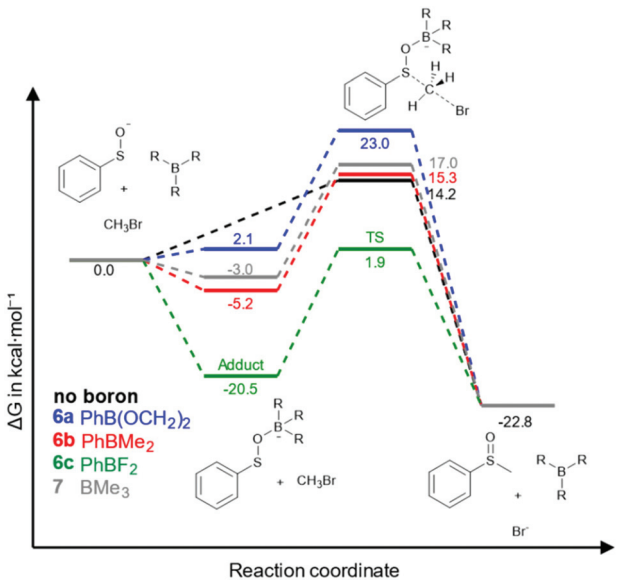

Fig. 8 Relative free energies of boron mediated sulfenate *S*-alkylations calculated at B3LYP/6-311++G(d,p); implicit solvation *via* CPCM(THF).

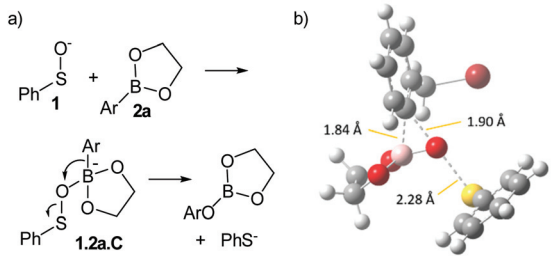

Fig. 9 (a) Possible mechanism for aryl to oxygen migration of boronate complex. (b) Transition state for aryl migration optimized with B3LYP/6-311++G(d,p); implicit solvation *via* CPCM(THF).

Finally, sulfenic acids and sulfenate esters have been recognized as 'thioperoxides' for a number of years.[29] As such they may be expected to participate in a hydroperoxide rearrangement that is an important component of the hydroboration/oxidation reaction sequence.[30] Indeed, chemistry demonstrated by the Yorimitsu group involves O → B complexes of sulfoxides and catB-Bcat, which subsequently break down by Bcat group migration from the ate complex to the oxygen while cleaving the O–S bond.[15]

A comparable reaction was viewed as feasible for the O → B complexes that are studied here (Fig. 9a), and such a reaction would be undesirable as it would compete with sulfenate alkylation. Accordingly, we sought to determine the free energy barrier for this migration. A suitable transition state was located for the migration of the 2-bromomethylphenyl group from boron to the sulfenate oxygen within **1·2a·C**, with concomitant loss of thiophenolate (Fig. 9b). Although the rearrangement pathway has an overall thermodynamic preference compared to sulfenate substitution (ΔG_r = −45.3 *vs.* −20.2 kcal mol^{-1}), its free energy of activation from precomplex **1·2a·C** of 29.4 kcal mol^{-1} is substantially higher than the sulfenate benzylation barrier of 8.7 kcal mol^{-1}. The findings clearly indicate the Ar migration will not compete with sulfenate alkylation.

Conclusions

This study employed computational tools to probe the role of proximal boron atoms in directing sulfenate *S*-alkylation chemistry. The work suggests there are cases where an intramolecularly positioned boronate atom can direct and accelerate a sulfenate *S*-alkylation event through initial precoordination of the sulfenate oxygen to the boron atom. This rate acceleration is mainly due to overcoming entropic barriers during complex formation and is highly dependent on the ring size involving the O → B complex in the *S*-alkylation transition state.

The use of intermolecular boron species led to sulfenate complexes that seemed to stabilize the sulfenate and reduce the rate of *S*-alkylation chemistry. A possible aryl migration mirroring a hydroperoxide rearrangement and involving the R–S–O–B–Ar linkage to release thiolate was found to be uncompetitive with sulfenate *S*-alkylation.

Given this work modelled the chemistry of sulfenate anions in the absence of an accompanying counterion, the effect of associated counterions on the rate of sulfenate alkylations remains undetermined. Nevertheless, our outcomes offer general features and guidance for practical experiments within the realm of sulfenate alkylation chemistry, and the concepts realized herein may also extend to other sulfenate functionalizations and to related nucleophiles such as sulfinate anions and those derived from H-phosphonates.

Conflicts of interest

There are no conflicts to declare.

Acknowledgements

The authors are grateful to Natural Sciences and Engineering Research Council (NSERC) of Canada for funding this research. EAN wish to thank the University of Guelph for a Guelph Excellence Entrance Scholarship. This research was enabled in part by support provided by SHARCNET (http://www.sharcnet.ca) and Compute Canada (http://www.compute-canada.ca).

Notes and references

1 (*a*) E. Block and M. Aslam, *Tetrahedron*, 1988, **44**, 281–324; (*b*) K. M. George and G. A. Molander, in *Comprehensive Organic Functional Group Transformations II*, ed. A. R. Katritzky and R. J. K. Taylor, Elsevier, Oxford, 2005, pp. 323–356; (*c*) N. G. Bhat, in *Comprehensive Organic Functional Group Transformations II*, ed. A. R. Katritzky and R. J. K. Taylor, Elsevier, Oxford, 2005, pp. 357–410; (*d*) J. Otera, T. Sato and H. Nozaki, in *Stereocontrolled Organic Synthesis*, ed. B. M. Trost, Blackwell, 1994, pp. 117–144.

2 B. L. Nilsson, L. L. Kiessling and R. T. Raines, *Org. Lett.*, 2000, **2**, 1939–1941.

3 F. Xu, L. Peng, K. Shinohara, T. Morita, S. Yoshida, T. Hosoya, A. Orita and J. Otera, *J. Org. Chem.*, 2014, **79**, 11592–11608.

4 K.-H. Huang, C.-C. Huang and M. Isobe, *J. Org. Chem.*, 2016, **81**, 1571–1584.

5 Z. J. Song, A. O. King, M. S. Waters, F. Lang, D. Zewge, M. Bio, J. L. Leazer Jr., G. Javadi, A. Kassim, D. M. Tschaen, R. A. Reamer, T. Rosner, J. R. Chilenski, D. J. Mathre, R. P. Volante and R. Tillyer, *Proc. Natl. Acad. Sci. U. S. A.*, 2004, **101**, 5776–5781.

6 (*a*) K. Wen, H. Wang, J. Chen, H. Zhang, X. Cui, C. Wei, E. Fan and Z. Sun, *J. Org. Chem.*, 2013, **78**, 3405–3409; (*b*) A. W. Buesking, V. Bacauanu, I. Cai and J. A. Ellman, *J. Org. Chem.*, 2014, **79**, 3671–3677.

7 (*a*) X. Li and D. G. Hall, *J. Am. Chem. Soc.*, 2020, **142**, 9063–9069; (*b*) X. Li and D. G. Hall, *Angew. Chem., Int. Ed.*, 2018, **57**, 10304–10308.

8 A. Fawcett, T. Biberger and V. K. Aggarwal, *Nat. Chem.*, 2019, **11**, 117–122.

9 A. Fawcett, A. Murtaza, C. H. U. Gregson and V. K. Aggarwal, *J. Am. Chem. Soc.*, 2019, **141**, 4573–4578.

10 G. Casoni, M. Kucukdisli, J. M. Fordham, M. Burns, E. L. Myers and V. K. Aggarwal, *J. Am. Chem. Soc.*, 2017, **139**, 11877–11886.

11 P. K. T. Lo and M. C. Willis, *J. Am. Chem. Soc.*, 2021, **143**, 15576–15581.

12 M. Čubiňák, V. Eigner and T. Tobrman, *Adv. Synth. Catal.*, 2018, **360**, 4604–4614.

13 N. Morohashi, T. Kitahara, T. Arima, S. Tanaka, Y. Ohba and T. Hattori, *Org. Lett.*, 2008, **10**, 2845–2848.

14 (*a*) H. C. Brown and N. Ravindran, *Synthesis*, 1973, 42–44; (*b*) S. Enthaler, S. Krackl, E. Irran and S. Inoue, *Catal. Lett.*, 2012, **142**, 1003–1010; (*c*) A. C. Fernandes and C. C. Romao, *Tetrahedron Lett.*, 2007, **48**, 9176–9179; (*d*) M. Madesclaire, *Tetrahedron*, 1988, **44**, 6537–6580; (*e*) H. Firouzabadi and A. Jamalian, *J. Sulfur Chem.*, 2008, **29**, 53–97.

15 F. Takahashi, K. Nogi and H. Yorimitsu, *Eur. J. Org. Chem.*, 2020, 3009–3012.

16 C. T. Liu and S. J. Benkovic, *J. Am. Chem. Soc.*, 2013, **135**, 14544–14547.

17 (*a*) A. L. Schwan and S. C. Soderman, *Phosphorus, Sulfur Silicon Relat. Elem.*, 2013, **188**, 275–286; (*b*) S. C. Söderman and A. L. Schwan, *J. Org. Chem.*, 2013, **78**, 1638–1649.

18 (*a*) C. Lee, W. Yang and R. G. Parr, *Phys. Rev. B: Condens. Matter Mater. Phys.*, 1988, **37**, 785–789; (*b*) P. J. Stephens, F. J. Devlin, C. F. Chabalowski and M. J. Frisch, *J. Phys. Chem.*, 1994, **98**, 11623–11627; (*c*) S. H. Vosko, L. Wilk and M. Nusair, *Can. J. Phys.*, 1980, **58**, 1200–1211; (*d*) A. D. Becke, *J. Chem. Phys.*, 1993, **98**, 5648–5652.

19 M. Gu and F. Turecek, *J. Am. Chem. Soc.*, 1992, **114**, 7146–7151.

20 J. W. Cubbage, Y. Guo, R. D. McCulla and W. S. Jenks, *J. Org. Chem.*, 2001, **66**, 8722–8736.

21 V. Barone and M. Cossi, *J. Phys. Chem. A*, 1998, **102**, 1995–2001.

22 (*a*) J. P. Foster and F. Weinhold, *J. Am. Chem. Soc.*, 1980, **102**, 7211–7218; (*b*) A. E. Reed, L. A. Curtiss and F. Weinhold, *Chem. Rev.*, 1988, **88**, 899–926.

23 C. F. Matta and R. J. Boyd, *The Quantum Theory of Atoms in Molecules*, Wiley–VCH Verlag, Weinheim, 2007.

24 (*a*) J.-F. Lohier, F. Foucoin, P.-A. Jaffrès, J. I. Garcia, J. Sopková-de Oliveira Santos, S. Perrio and P. Metzner, *Org. Lett.*, 2008, **10**, 1271–1274; (*b*) F. Foucoin, C. Caupene, J.-F. Lohier, J. S. d. O. Santos, S. Perrio and P. Metzner, *Synthesis*, 2007, 1315–1324.

25 (*a*) B. Carboni and L. Monnier, *Tetrahedron*, 1999, **55**, 1197–1248; (*b*) I. B. Sivaev and V. I. Bregadze, *Coord. Chem. Rev.*, 2014, **270–271**, 75–88.

26 D. G. Hall, *Boronic Acids. Volume 2. Preparation and Applications in Organic Synthesis*, *Medicine and Materials*, Wiley-VCH Verlag, Weinheim, 2011.
27 E. Uggerud, in *Advances in Physical Organic Chemistry*, ed. I. H. Williams and N. H. Williams, Academic Press, 2017, vol. 51, pp. 1–57.
28 A. L. Schwan, *Eur. J. Org. Chem.*, 2019, 519–526.
29 (*a*) M. A. Hardy, H. Chachignon and D. Cahard, *Asian J. Org. Chem.*, 2019, **8**, 591–609; (*b*) R. S. Irwin and N. Kharasch, *J. Am. Chem. Soc.*, 1960, **82**, 2502–2505; (*c*) S. V. Makarov, A. K. Horváth and A. S. Makarova, *Molecules*, 2019, **24**, 2768.
30 G. Zweifel and H. C. Brown, *Org. React.*, 1963, **13**, 1–54.
31 M. J. Frisch, G. W. Trucks, H. B. Schlegel, G. E. Scuseria, M. A. Robb, J. R. Cheeseman, G. Scalmani, V. Barone, G. A. Petersson, H. Nakatsuji, X. Li, M. Caricato, A. V. Marenich, J. Bloino, B. G. Janesko, R. Gomperts, B. Mennucci, H. P. Hratchian, J. V. Ortiz, A. F. Izmaylov, J. L. Sonnenberg, D. Williams-Young, F. Ding, F. Lipparini, F. Egidi, J. Goings, B. Peng, A. Petrone, T. Henderson, D. Ranasinghe, V. G. Zakrzewski, J. Gao, N. Rega, G. Zheng, W. Liang, M. Hada, M. Ehara, K. Toyota, R. Fukuda, J. Hasegawa, M. Ishida, T. Nakajima, Y. Honda, O. Kitao, H. Nakai, T. Vreven, K. Throssell, J. A. Montgomery Jr., J. E. Peralta, F. Ogliaro, M. J. Bearpark, J. J. Heyd, E. N. Brothers, K. N. Kudin, V. N. Staroverov, T. A. Keith, R. Kobayashi, J. Normand, K. Raghavachari, A. P. Rendell, J. C. Burant, S. S. Iyengar, J. Tomasi, M. Cossi, J. M. Millam, M. Klene, C. Adamo, R. Cammi, J. W. Ochterski, R. L. Martin, K. Morokuma, O. Farkas, J. B. Foresman and D. J. Fox, *Gaussian 16, Revision.b01*, Gaussian, Inc., Wallingford CT, 2016.
32 E. D. Glendening, J. K. Badenhoop, A. E. Reed, J. E. Carpenter, J. A. Bohmann, C. M. Morales, C. R. Landis and F. Weinhold, *NBO 6.0*, Theoretical Chemistry Institute, University of Wisconsin, Madison WI, 2013.
33 S. Grimme, *WIREs Comput. Mol. Sci.*, 2011, **1**, 211–228.
34 H. Kruse, L. Goerigk and S. Grimme, *J. Org. Chem.*, 2012, **77**, 10824–10834.